Breather scattering by impurities in the sine-Gordon model

Fei Zhang
Department of Computational Science, Faculty of Science, National University of Singapore, Singapore 119260
(Received 11 November 1997; revised manuscript received 31 March 1998)

We present results on breather-impurity scattering in the sine-Gordon model. We show in detail how the outcome of the scattering depends on the breather's initial velocity, internal oscillation frequency, and phase. In particular, for an attractive impurity a breather can either be trapped by the impurity, pass the impurity, be totally *reflected*, or break into a kink-antikink pair. For a repulsive impurity, a high-frequency breather behaves like a rigid particle and the scattering result is mainly determined by the breather's initial velocity; the scattering of a low-frequency breather, however, depends on both the breather's initial velocity and phase (it can either pass the impurity or be reflected for a fixed initial velocity but different phases). We demonstrate clearly that the existence of these complex and interesting phenomena is due to the interplay between the breather's internal and its translational degrees of freedom, which become strongly coupled when the breather is near the impurity region. [S1063-651X(98)02908-0]

PACS number(s): 03.40.Kf, 63.50.+x, 66.90.+r

I. INTRODUCTION

Nonlinear wave (soliton) propagation through inhomogeneous and disordered media is an important area of current research. In particular, the issue how the steady-state motion of solitons can be qualitatively modified by the presence of impurity perturbations is of widespread interest [1–12]

Due to its practical application and analytical tractability, the sine-Gordon (SG) model has been serving as a paradigm for studying solitons behavior under perturbations. Many early analytical studies were based on inverse-scattering perturbation theory [3–7]. This theory is a bit involved and not easily accessible, thus other simpler methods have also been developed [8,9]. In particular, recently Mann [9] has developed a systematic perturbation theory for SG solitons without the use of inverse-scattering methods. We note that while these analytical approaches can often provide useful insights, they generally cannot give a detailed and accurate picture about soliton dynamics under perturbations. In this situation, direct numerical simulation of the full problem (described by a partial differential equation) is a powerful alternative method for studying the soliton dynamics. In particular, it can be used to check the analytical results and to reveal different phenomena [10,11].

The problem of breather-impurity interaction in the SG model was briefly studied in Refs. [6,8] by using inverse-scattering perturbation theory and the collective-coordinate approach. However, due to the limitation of their analytical approaches, previous researchers could obtain only a small fraction of the overall picture of breather-impurity interaction dynamics. Many interesting phenomena were missing. The objective of the present paper is to show that the breather-impurity interactions exhibit *much more complex and striking dynamics than previously indicated*. We demonstrate that the breather's internal and translational degrees of freedom become strongly coupled when it is near the impurity and such a coupling makes it possible to transfer a significant amount of energy between the breather's internal oscillation and its translational motion; as a result, the breather's velocity and frequency can be changed drastically after the scattering. In the case of an attractive impurity, there are four types of scattering outcome: breather (i) passing, (ii) trapping, (iii) reflection, and (iv) breaking into a kink-antikink pair *even when the breather's initial energy is less than 16* (double the energy of a kink at rest). In the case of repulsive impurity, a low-frequency breather may either pass or be reflected by the impurity, depending on both the breather's velocity and internal phase; the scattering of a high-frequency breather depends mainly on the breather's initial velocity and is not sensitive to its initial phase. These results are obtained through direct numerical simulations of the perturbed SG system and they can be understood with the help of a simple collective-coordinate approach.

II. COLLECTIVE-COORDINATE ANALYSIS

We consider the perturbed SG model

$$\phi_{tt}-\phi_{xx}+[1+\epsilon U(x)]\sin\,\phi=0, \tag{1}$$

where $\epsilon U(x)$ represents a local impurity. Such a model can be used to describe many physical systems including long Josephson junctions with microshunts and microresistors. See, e.g., Refs. [3–13]. The unperturbed SG equation has a breather solution [14]

$$\phi_B(x,t)=4\tan^{-1}\left\{\tan\,\mu\,\frac{\sin\left[q_1(t)-\dfrac{Vx\,\cos\,\mu}{\sqrt{1-V^2}}\right]}{\cosh\left[\dfrac{x\,\sin\,\mu-q_2(t)}{\sqrt{1-V^2}}\right]}\right\}, \tag{2}$$

which is characterized by two pairs of action-angle-type canonical variables: $(p_1=M\mu,q_1)$ and $(p_2=MV/\sqrt{1-V^2},q_2)$, where $M=16$ and V is the breather's velocity.

To analyze breather-impurity interactions one can use a collective-coordinate approach, assuming that the major effect of the interactions is a change of the breather's parameters. Then the perturbed Hamiltonian is (see Refs. [6,8])

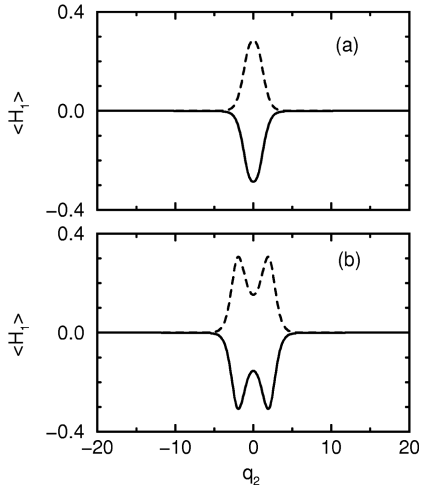

FIG. 1. Average Hamiltonian $\langle H_1 \rangle$ vs the breather's position coordinate q_2. Solid lines, attractive impurity $\epsilon = -0.2$; dashed lines, repulsive impurity $\epsilon = 0.2$. The breather's frequencies are (a) $\Omega = 0.7 > \Omega_c$ and (b) $\Omega = 0.2 < \Omega_c$.

$$H \equiv H(p_1, p_2, q_1, q_2) = H_B + H_1, \tag{3}$$

where H_B corresponds to the unperturbed Hamiltonian (or energy) for the breather

$$H_B = \sqrt{M^2 + p_2^2} \sin \frac{p_1}{M} \tag{4}$$

and

$$H_1 = 8\epsilon \left[\frac{\tan(p_1/M) \sin q_1 \cosh[q_2 \sqrt{1 + (p_2/M)^2}]}{\tan^2(p_1/M) \sin^2 q_1 + \cosh^2[q_2 \sqrt{1 + (p_2/M)^2}]} \right]^2. \tag{5}$$

[Here the localized impurity is represented by a delta function $U(x) = \delta(x)$.]

In order to understand the qualitative effect of the perturbation, one can calculate the average of H_1 over a period of the breather's internal oscillation [6]

$$\langle H_1 \rangle = 4\epsilon \tan^2\left(\frac{p_1}{M}\right) \cosh[q_2 \sqrt{1 + (p_2/M)^2}] \left\{ \tan^2\left(\frac{p_1}{M}\right) + \cosh^2[q_2 \sqrt{1 + (p_2/M)^2}] \right\}^{-3/2}. \tag{6}$$

Therefore, for a given breather's velocity (or momentum p_2), the average potential depends on the breather's position and frequency $\Omega = \cos(p_1/M)$. In particular, there exists a critical breather frequency $\Omega_c = 1/\sqrt{3}$ such that the shape of the average potential is qualitatively different for the case of $\Omega < \Omega_c$ and the case of $\Omega > \Omega_c$ (see Fig. 1). Moreover, if $\epsilon < 0$, then the impurity can create an attractive potential (single or double well) to a breather and thus a high-velocity breather will be able to pass the impurity, but a low-velocity breather may be trapped due to radiative losses of its translational energy during the scattering. If $\epsilon > 0$, then the impurity is purely repulsive to a high-frequency breather ($\Omega > \Omega_c$), so that a low-velocity breather will be reflected by the impurity and a high-velocity breather will pass. A low-frequency breather ($\Omega < \Omega_c$), on the other hand, experiences a metastable state in the average potential so that it may be trapped at the impurity. These results were also indicated in Refs. [6,8]. In the following we will use numerical simulations to reveal many additional effects that are far more interesting.

Note that the canonical equations of motion derived from Eq. (3) are highly singular when $\mu = p_1/M \approx \pm \pi/2$ (because of zero denominators), i.e., when a breather breaks into a kink-antikink pair. The presence of such singular phase points can cause a ''blowup'' in numerical simulations. To overcome this difficulty we make a change of variable $\bar{p}_1 = \tan(p_1/M)$ and transform the Hamiltonian equations into the system of ordinary differential equations

$$\frac{d\bar{p}_1}{dt} = -8\epsilon W \sin(2q_1) \cosh^2(\gamma q_2) \bar{p}_1^2 (1 + \bar{p}_1^2)/M, \tag{7}$$

$$\frac{dq_1}{dt} = \gamma / \sqrt{1 + \bar{p}_1^2} + \epsilon W \sin^2(q_1) \cosh^2(\gamma q_2) \bar{p}_1 (1 + \bar{p}_1^2), \tag{8}$$

$$\frac{dp_2}{dt} = 8\epsilon \gamma W \bar{p}_1^2 \sin^2(q_1) \sinh(2\gamma q_2), \tag{9}$$

$$\frac{dq_2}{dt} = \frac{\bar{p}_1 p_2}{M\gamma \sqrt{1 + \bar{p}_1^2}} - \frac{\epsilon W \bar{p}_1^2 p_2 q_2 \sin^2(q_1) \sinh(2\gamma q_2)}{2M\gamma}, \tag{10}$$

where

$$\gamma = \sqrt{1 + (p_2/M)^2}$$

and

$$W = [\cosh^2(\gamma q_2) - \bar{p}_1^2 \sin^2(q_1)][\cosh^2(\gamma q_2) + \bar{p}_1^2 \sin^2(q_1)]^{-3}.$$

We supply the initial values for $(\bar{p}_1, q_1, p_2, q_2)$ in accordance with a breather with a given initial velocity V, frequency Ω, fixed position $X_0 = -20$, and 30 different initial phases ranging from 0 to π, i.e., $q_1(0) = k\pi/30$, $k = 1,2,\ldots,30$. [Note that the Hamiltonian H_1 is π periodic in q_1; thus we only need to consider the initial phase in $(0,\pi)$.] The simulation results are summarized as follows.

In the case of an attractive impurity ($\epsilon < 0$), we take $\epsilon = -0.5$. In the simulations we find that for a given initial velocity and frequency, the outcome of breather scattering depends strongly on the the breather's initial phase $q_1(0)$. In particular, a low-velocity breather may either pass the impurity or be reflected by the impurity. In this case the final velocity (and thus frequency) of the breather may be altered significantly (see Fig. 2). In some cases, we observe long-time trapping of the breather by the impurity potential, although such trapping might be transient (see Fig. 3).

Another striking effect of the scattering is that a low-frequency breather may break into a kink-antikink ($K\bar{K}$) pair *even when its energy is less than 16*. This is evidenced by the

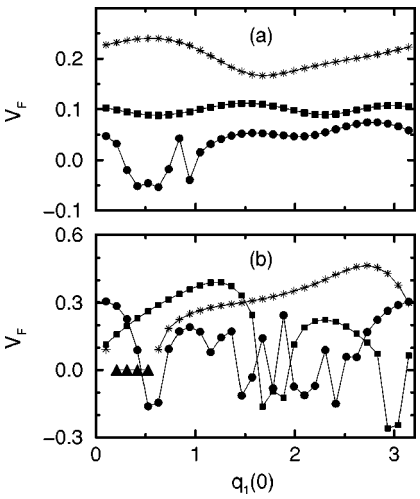

FIG. 2. Final velocity of the breather vs its initial phase, for the case of an attractive impurity $\epsilon=-0.5$. The breather's frequencies and velocities are (a) $\Omega=0.6$, $V=0.05$ (circles), $V=0.1$ (squares), and $V=0.2$ (asterisks) and (b) $\Omega=0.4$, $V=0.1$ (circles), $V=0.2$ (squares), and $V=0.3$ (asterisks). Note that the four triangles in (b) indicate the breaking of breather into a kink-antikink pair for $V=0.3$. See the text.

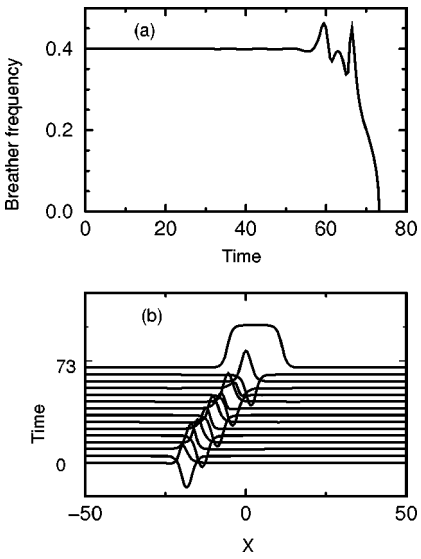

FIG. 4. Collective-coordinate results ($\epsilon=-0.5$), showing that (a) a breather frequency goes to zero and (b) it breaks into a kink-antikink pair. The field configuration in (b) is obtained by substituting the collective coordinate results into the ansatz (2). The breather initial conditions are $\Omega=0.4$, $V=0.3$, and $q_1(0)=\pi/10$.

fact that the variable $\overline{p_1}$ becomes ''infinite'' (the breather's frequency approaches to zero) and the breather ansatz (2) clearly becomes a $K\overline{K}$ pair (Fig. 4).

To understand why a breather can break into a $K\overline{K}$ pair even when its energy is less than the minimum energy of an unbounded $K\overline{K}$ pair, we note that the attractive impurity can create an effective potential well of depth $2|\epsilon|$ to a kink (or antikink) [10,11]. Therefore, from an energetics point of view, the critical condition for a breather to be converted into a $K\overline{K}$ pair is ($\epsilon<0$)

$$E_B \equiv \frac{16\sqrt{1-\Omega^2}}{\sqrt{1-V^2}} = 16+2\epsilon. \tag{11}$$

Note that the left-hand side of Eq. (11) is just the energy of the breather. Solving this equation, we can get a critical velocity $V_c=V_c(\Omega,\epsilon)$. For example, at $\epsilon=-0.5$ and $\Omega=0.4$, Eq. (11) gives $V_c\approx 0.2104$. Indeed, we observe that the breather with initial velocity $V=0.3$ is broken into a $K\overline{K}$ pair for the initial phases $q_1(0)=k\pi/30$, $k=2,3,4,5$ [see Figs. 2(b) and 4].

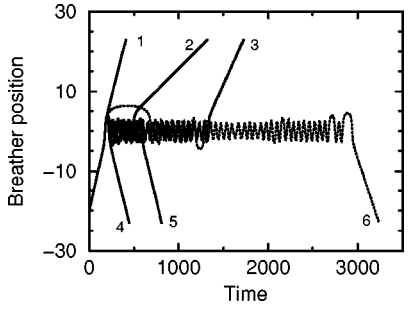

FIG. 3. Breather location vs time, obtained by the collective coordinate approach for the impurity parameter $\epsilon=-0.5$. The breather frequency and velocity are $\Omega=0.5$ and $V=0.1$, respectively, and its initial phases are $q_1(0)=k\pi/30$, with $k=21$, 26, 29, 24, 25, and 30 for curves 1, 2, 3, 4, 5, and 6, respectively.

In the case of a repulsive impurity ($\epsilon>0$), the scattering of a high-frequency breather ($\Omega>1/\sqrt{3}$) depends very little on the initial phase. The breather behaves like a rigid particle of mass $16\sqrt{1-\Omega^2}$ interacting with a repulsive potential. Whether or not it can pass the impurity depends only on whether it has enough energy to overcome the potential barrier. Using an energy argument, we find that the critical velocity of the breather passing can be estimated as $V_c=\sqrt{0.5\epsilon\Omega\sqrt{1-\Omega^2}}$. For example, at $\epsilon=0.1$ and $\Omega=0.9$, this equation gives $V_c=0.140$. In numerical simulations, we observe that a breather will always pass the impurity for $V\geqslant 0.1386$, but it will be reflected for $V\leqslant 0.1385$. In both cases, the final breather's frequency and velocity (absolute value) are virtually unchanged.

For a low-frequency breather ($\Omega_B<1/\sqrt{3}$), the scattering is more complicated because of the existence of the *metastable* state in the average potential $\langle H_1\rangle$. For a given impurity strength ϵ, there exists a critical velocity V_{c1} such that if the breather's incoming velocity is smaller than V_{c1} then it will be reflected (for all phases). Again using an energy argument we find $V_{c1}\approx 3^{-3/4}\sqrt{\epsilon/\sqrt{1-\Omega^2}}$. Furthermore, there exists another critical velocity V_{c2} ($>V_{c1}$), above which the breather will always pass the impurity.

Interestingly, for the breather velocity in the interval $[V_{c1},V_{c2}]$, there are possibilities of passing, reflection, and even long-time trapping into the metastable state. For example, at $\epsilon=0.1$ and $\Omega_B=0.2$, we find in numerical simulations that if the breather's initial velocity is smaller than $V_{c1}=0.137$, then it will always be reflected; if it is larger than $V_{c2}=0.158$, then it will always pass the impurity. If the breather's initial velocity is located in the interval [0.137, 0.158], then it may either pass the impurity or be reflected,

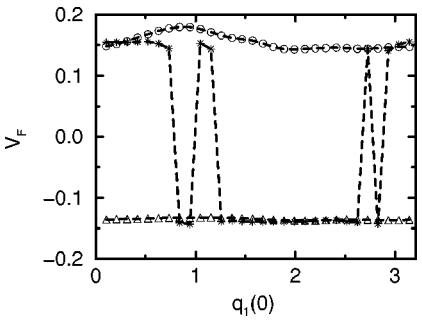

FIG. 5. Final velocity of a breather with initial frequency $\Omega = 0.2$ vs its initial phase, for the case of a repulsive impurity $\epsilon = 0.1$. The breather's initial velocities are $V = 0.136$ (triangles), $V = 0.140$ (asterisks), and $V = 0.158$ (circles).

depending on the breather's *initial phase* (Fig. 5).

For a repulsive impurity, a low-frequency breather may be broken into a kink-antikink pair only when its initial energy is *greater than 16* (in contrast to the case of an attractive impurity). For example, at $\epsilon = 0.1$ and $\Omega = 0.1$, it is found that the breather will always be reflected if its initial velocity $V \leqslant 0.1$; otherwise ($V \geqslant 0.11$), it can break into kink-antikink pair for some initial phases.

III. DIRECT NUMERICAL SIMULATION RESULTS

We carry out detailed numerical simulations of the perturbed SG system (1) in the spatial interval $[-100,100]$ with free boundary conditions. Unlike in the previous works [10,11] where the δ impurity is approximated by a discontinuous step function, here we use a continuous function

$$\epsilon U(x) = \frac{\alpha}{\cosh^2(x/\beta)} \tag{12}$$

to represent the impurity of width β. Note that when β goes to zero the right-hand side of Eq. (12) approaches $2\alpha\beta\delta(x)$. A simple second-order central difference scheme is used to discretize the equation in space with step size $\Delta x = 0.02$ and then a fourth-order symplectic method [15] is used to integrate the resulting discrete Hamiltonian model in time with temporal step size $\Delta t = 0.01$.

The initial conditions are taken as an exact breather (2) with a fixed initial position $X_0 = -20$ [$q_2(0) = X_0 \sin(\mu)$], an initial frequency $\Omega = \cos(\mu)$ and velocity V, and 30 *different phases* $q_1(0) = k\pi/30$, $k = 1,2, \ldots, 30$.

First, we consider a *very localized* attractive impurity with the parameters $\beta = 0.04$ $\alpha = -6.25$. This is close to a δ impurity with strength $\epsilon = 2\alpha\beta = -0.5$. In numerical simulations, we observe that a low-frequency breather can either pass, be reflected, be trapped, or break into a $K\overline{K}$ pair, depending on its initial frequency, velocity, and phase. For instance, taking the breather parameters as $\Omega = 0.4$, $V = 0.35$, and $q_1(0) = k\pi/30$, we find that it is trapped by the impurity for the initial phase with $k = 1$, breaks into a $K\overline{K}$ pair for $k = 2$ and 3, is reflected for $k = 4$, and passes the impurity for initial phases with $5 \leqslant k \leqslant 30$. See Fig. 6. In the cases of passing and reflection, the breather's final velocity and frequency depend strongly on the breather's initial phase and they can be changed a lot from their initial values, just as has been predicted in the collective-coordinate approach.

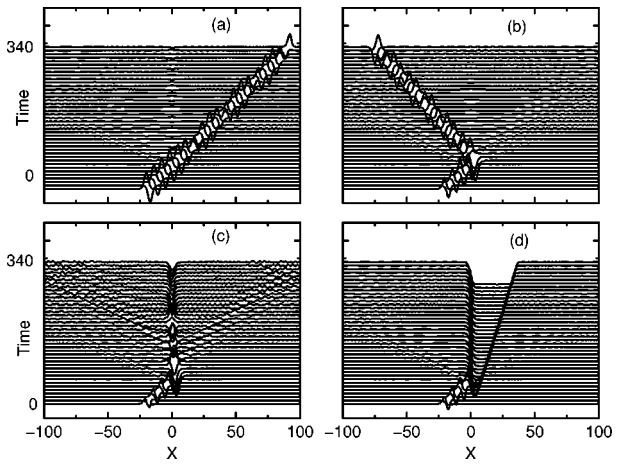

FIG. 6. Evolution of the field $\phi(x,t)$ for a breather with initial frequency $\Omega = 0.4$, velocity $V = 0.35$, and different initial phases, scattered by an attractive impurity. The breather (a) passes the impurity for phase $q_1(0) = \pi/2$, (b) is reflected for $q_1(0) = 2\pi/15$, (c) is trapped for $q_1(0) = \pi/30$, and (d) decays into a kink-antikink pair for $q_1(0) = \pi/15$. (The antikink is trapped at the impurity and the kink moves forward.)

For a breather with an intermediate frequency, we find that it can always pass the impurity if its initial velocity is large enough; but it may either pass, be trapped, or be reflected if its initial velocity is low. For example, taking the breather frequency as $\Omega = 0.6$, we find that it can always pass the impurity if $V \geqslant 0.1$. However, at the initial velocity $V = 0.05$, the breather may pass the impurity for most initial phases, while it can be either trapped or reflected for some other phases (Fig. 7).

We note that the attractive impurity can support a localized impurity mode, which can be considered as a *small-amplitude* breather trapped by the impurity. In linear limit, the frequency of the impurity mode is $\omega_{im} = \sqrt{1 - \epsilon^2/4}$. (See Refs. [10,11].) When the scattering breather's frequency is close to this impurity mode's frequency, the scattering can strongly excite the impurity mode. In this case, the collective-coordinate approach is no longer valid because it does not take into account the impurity mode. In the direct numerical simulations we study the scattering of a breather with frequency $\Omega = 0.9$ (which is close to the impurity mode frequency 0.968) and we find that, no matter what the phase is, the breather will be trapped if its initial velocity is small ($\leqslant 0.25$) and it will pass the impurity if its initial velocity is sufficiently large. A lot of radiation is generated due to the breather-impurity interactions (see Fig. 8) and the breather cannot be reflected nor break into a $K\overline{K}$ pair.

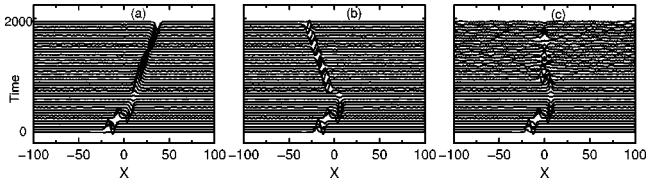

FIG. 7. Evolution of the field $\phi(x,t)$ for a breather with initial frequency $\Omega = 0.6$, velocity $V = 0.05$, and different initial phases, scattered by an attractive impurity. The breather (a) passes the impurity for phase $q_1(0) = 0$, (b) is reflected for $q_1(0) = 9\pi/10$, and (c) is trapped for $q_1(0) = 14\pi/15$.

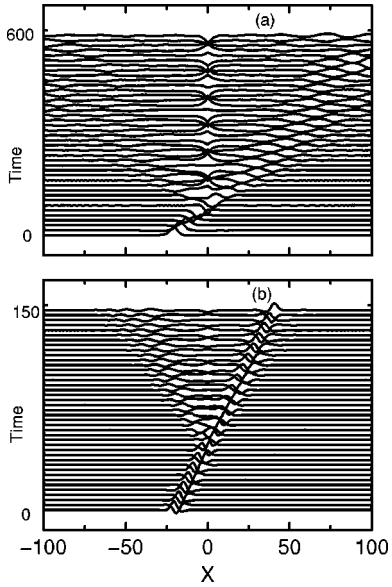

FIG. 8. Evolution of the field $\phi(x,t)$ for a breather with initial frequency $\Omega=0.9$, scattered by an attractive impurity. The breather (a) is trapped at the impurity for initial velocity $V=0.2$ and $q_1(0)=\pi/3$ and (b) passes at $V=0.4$ and $q_1(0)=\pi/3$.

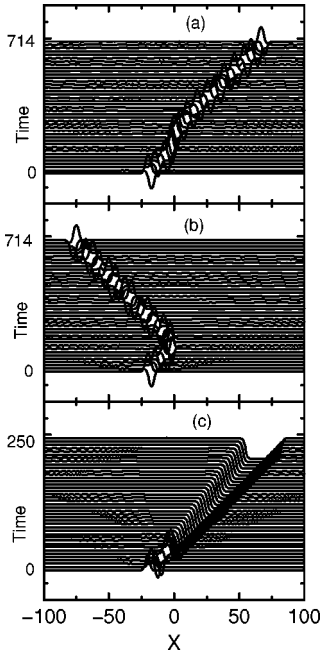

FIG. 9. Evolution of the field $\phi(x,t)$ for a breather with frequency $\Omega=0.2$, scattered by a repulsive impurity. The breather (a) passes for $V=0.14$ and $q_1(0)=16\pi/30$, (b) is reflected for $V=0.14$ and $q_1(0)=17\pi/30$, and (c) breaks into a kink-antikink pair for $V=0.4$ and $q_1(0)=\pi/6$.

In the case of repulsive impurity, we take $\alpha=1.25$ and $\beta=0.04$ $[\epsilon U(x)\approx 2\alpha\beta\delta(x)=0.1\delta(x)]$. For a high-frequency breather, we observe that there exists a critical velocity V_c such that for any initial phase, the breather can pass the impurity if its initial velocity exceeds V_c and it will be reflected if its initial velocity is less than V_c. As an example, we take $\Omega=0.8$. We observe in numerical simulations that the breather always passes if its initial velocity is greater than 0.153 and it will be reflected otherwise. This is in good agreement with collective-coordinate prediction (Sec. II), which gives $V_c=0.155$.

For a low-frequency breather scattering, the results also turn out to be in good agreement with the collective coordinate approach. We simulate a breather with $\Omega=0.2$ and find that for any initial phase if the breather's initial velocity is less than 0.137 it will be reflected; if its initial velocity is greater than 0.148 it will pass. However, when the breather's initial velocity is in between 0.137 and 0.148, the scattering results will depend sensitively on the breather's initial phase. In particular, for a given initial velocity (e.g., $V=0.14$), the breather can pass the impurity for some phases and it can be reflected for some other phases (Fig. 9). Moreover, if the breather's initial velocity is high enough ($\geqslant 0.4$), then it can break into a $K\bar{K}$ pair. See Fig. 9(c). We have also studied breather scattering by a large-size impurity (e.g., $\beta=2$) and found that the results are similar to those obtained above for a δ-like impurity.

IV. CONCLUSIONS

Table I encapsulates the major effects observed in soliton-impurity scattering in the sine-Gordon model. We would like to emphasize that in contrast to the resonant kink-impurity interactions where the impurity mode plays an important role [10,11], the rich dynamics in breather scattering is due to the

TABLE I. Summary of soliton-impurity interactions in the sine-Gordon model.

Impurity type	Attractive impurity	Repulsive impurity
kink	resonance structures[a]	no resonance structures[a]
low-frequency breather	either pass or trap[b]	either pass or reflection depending on only velocity[b]
	decay into $K\bar{K}$ pair for $E_b \gg 16$[c]	both velocity and phase[d]
	reflection[d]	decay into $K\bar{K}$ pair for $E_b \gg 16$[c]
	decay into $K\bar{K}$ pair for $E_b < 16$[d]	
high-frequency breather	either pass or trap[b]	either pass or reflection[b]
	excitation of impurity mode[d]	

[a]References [10,11]
[b]References [6,8].
[c]Reference [6].
[d]Present results.

interplay between the breather's own (internal oscillation and translation) degrees of freedom. When near the impurity a breather experiences an effective potential and its degrees of freedom become strongly coupled. As a result, it may either pass the impurity, be reflected, be trapped, or even break into a kink-antikink ($K\bar{K}$) pair. The outcome of scattering depends not only on the breather's velocity and frequency, but also on the breather's initial *phases*. Most strikingly, in the case of an attractive impurity, the decay of a low-frequency breather into a $K\bar{K}$ pair may occur even when the breather's initial energy E_b is less than 16. We believe that similar phenomena can be observed in the SG model with other types of perturbation.

ACKNOWLEDGMENTS

I thank Yuri Kivshar for useful discussions. This work was supported by Academic Research Grants Nos. 950601 and 960689 and by the Lee Kuan Yew Endowment Fund in the National University of Singapore.

[1] *Nonlinearity with Disorder*, edited by F. Kh. Abdullaev, A. R. Bishop, and St. Pnevmatikos (Springer-Verlag, Berlin, 1992); *Fluctuation Phenomena: Disorder and Nonlinearity*, edited by A. R. Bishop, S. Jimenez, and L. Vázquez (World Scientific, Singapore, 1995); F. Abdullaev, *Theory of Solitons in Inhomogeneous Media* (Wiley, Chichester, 1994).

[2] R. Scharf and A. R. Bishop, Phys. Rev. A **43**, 6535 (1991); K. Forinash, M. Peyrard, and B. A. Malomed, Phys. Rev. E **49**, 3400 (1994); K. Fukushima and T. Yamada, Phys. Lett. A **200**, 350 (1995); V. V. Konotop *et al.*, Phys. Rev. E **53**, 6476 (1996); G. Kalbermann, *ibid.* **55**, R6360 (1997).

[3] D. W. Mclaughlin and A. C. Scott, Phys. Rev. A **18**, 1652 (1978).

[4] D. J. Kaup and A. C. Newell, Proc. R. Soc. London, Ser. A **361**, 413 (1978).

[5] V. I. Karpman and V. V. Solov'ev, Phys. Lett. **84A**, 39 (1981); V. I. Karpman, E. M. Maslov, and V. V. Solov'ev, Sov. Phys. JETP **57**, 167 (1983).

[6] B. A. Malomed, Physica D **15**, 385 (1985); **27**, 113 (1987).

[7] Yu. S. Kivshar and B. A. Malomed, Rev. Mod. Phys. **61**, 763 (1989).

[8] E. V. Gurovich and V. G. Mikhalev, Sov. Phys. JETP **66**, 731 (1987).

[9] E. Mann, J. Phys. A **30**, 1227 (1997).

[10] Yu. S. Kivshar, F. Zhang, and L. Vázquez, Phys. Rev. Lett. **67**, 1177 (1991).

[11] F. Zhang, Yu. S. Kivshar, and L. Vázquez, Phys. Rev. A **45**, 6019 (1992); **46**, 5214 (1992).

[12] N. Burroughs, Physica D **101**, 95 (1997).

[13] A. A. Golubov, I. L. Serpuchenko, and A. V. Ustinov, Sov. Phys. JETP **67**, 1256 (1988).

[14] S. Novikov *et al.*, *Theory of Solitons: The Inverse Scattering Methods* (Consultants Bureau, New York, 1984); L. D. Faddeev and L. A. Takhtajan, *Hamiltonian Methods in the Theory of Solitons* (Springer-Verlag, Berlin, 1987).

[15] J. M. Sanz-Serna and M. P. Calvo, *Numerical Hamiltonian Problems* (Chapman & Hall, London, 1994); F. Zhang, Comput. Phys. Commun. **99**, 53 (1996).